Deletion of Calponin 2 Reduces the Formation of Postoperative Peritoneal Adhesion

Tzu-Bou Hsieh[1], **Han-Zhong Feng**[2], **Jian-Ping Jin**[1,2]

[1]Department of Obstetrics and Gynecology, Wayne State University School of Medicine, Detroit, Michigan 48201, USA

[2]Department of Physiology, Wayne State University School of Medicine, Detroit, Michigan 48201, USA

Abstract

Postoperative peritoneal adhesions are a common cause of morbidity, resulting in multiple complications. Macrophage-mediated inflammation and myofibroblast differentiation after tissue injury play central roles in the pathogenesis and progression. Calponin 2 is an actin cytoskeleton regulatory protein in endothelial cells, macrophages and fibroblasts that are key players in the development of postoperative peritoneal adhesion. Deletion of calponin 2 has been shown to attenuate inflammatory arthritis, atherosclerosis and fibrocalcification of aortic valve. The present study investigated the effect of calponin 2 deletion on attenuating the formation of peritoneal adhesion in a mouse model for potential use as a new therapeutic target. A sterile surgical procedure under general anesthesia was used on paired wild type (WT) and calponin 2 knockout (KO) mice to generate mild injury on cecal and abdominal wall peritonea. Three and seven days post-operation, the mice were compared post-mortem for the formation of peritoneal adhesions. Tissues at the adhesion sites were examined with histology and immunofluorescent studies for macrophage and myofibroblast activations. Quantitative scoring demonstrated that calponin 2 KO mice developed significantly less postoperative peritoneal adhesion than that in WT mice. Calponin 2 deletion resulted in less infiltration of F4/80$^+$ macrophages at the adhesion sites with less myofibroblast differentiation and collagen deposition than WT controls. The data show that deletion of calponin 2 effectively reduces postoperative peritoneal adhesion, presenting a novel molecular target for clinical prevention.

Keywords

calponin 2; myofibroblast; inflammation; adhesions

Introduction

Postsurgical peritoneal adhesion is a common clinical complication caused by operational injuries during abdominal surgeries including sterile procedures[1]. The pathogenesis starts with inflammatory responses and wound healing, leading to the formation of fibrotic adhesion between abdominal organs[2, 3]. Such adhesion is nearly always permanent and constitutes a major health problem that commonly occurs after surgeries, subjecting the patients to a lifelong risk of various secondary disorders[4]. The iatrogenic complications include chronic pain, small bowel obstruction, difficulties in reoperation and female infertility[5].

Surgical procedures are invasive and produce tissue lesions that promote inflammatory responses followed with repair including fibrotic remodeling. The formation of peritoneal adhesion post-abdominal surgeries is of high occurrence, relating to the extent and frequency of surgical procedures. For example, a study found adhesions in 24.4% of women when undergone second cesarean section and 42.8% when undergone third cesarean section[6]. Postoperative adhesions cause a major economic burden in healthcare. It was estimated that the direct hospital costs of adhesiolysis-related procedures was ~$2.3 billion in the United States in 2005[7].

New surgical techniques such as minimally invasive surgery and anti-adhesion barriers have been developed to prevent adhesion formation. However, a comprehensive review in 2019 concluded that neither adhesion barriers nor laparoscopic adhesiolysis surgery actually reduced the formation of peritoneal adhesion in animal models[8]. More research is needed to timely identify new molecular targets and approaches to the prevention and attenuation of postoperative peritoneal adhesion.

The pathogenesis of peritoneal adhesion after traumatic tissue injuries during surgery involves inflammation, wound healing, and tissue remodelling[9]. Postoperative inflammatory response and tissue repair have a high tendency to cause the formation of peritoneal adhesion. The inflammatory responses start in minutes with platelets accumulation and activation of coagulation cascade to form fibrin meshes covering the injured area. In the following hours, the denuded connective tissue beds are infiltrated with macrophages and the underneath fibroblasts start to proliferate for repairing the injured tissue. Excessive inflammatory response and fibroblast activation would lead to the formation of permanent fibrosis and adhesions[10, 11]. During the inflammatory stage, macrophages play a central role in orchestrating innate immune response. Cytokines and growth factors released from the macrophages activate fibroblasts transformed from mesothelial cells, a process known as mesothelial-to-mesenchymal transition (MMT)[11, 12] to differentiate into myofibroblasts with contractile phenotypes. Therefore, macrophage-mediated inflammatory response and myofibroblast differentiation are major components of the pathogenesis and progression of postoperative peritoneal adhesion.

Calponin is an actin-binding protein that regulates the structure and function of actin cytoskeleton through inhibiting actin-activated myosin ATPase and motor activities[13–15]. Three isoforms of calponin, calponins 1, 2, and 3, are present in vertebrates encoded by

homologous genes, *Cnn1, Cnn2, and Cnn3,* respectively[16, 17]. Calponin 1 is expressed exclusively in smooth muscle and functions to regulate smooth muscle contractility[16, 18–20]. Calponin 2 is expressed in smooth muscles and in non-muscle cells such as epithelial cells, endothelial cells, myeloid blood cells and fibroblasts[18, 21, 22] with functions in regulating cell proliferation, adhesion, migration and phagocytosis[16, 17]. Calponin 3 is found in smooth muscle, brain, trophoblasts, and B-lymphocytes with a function of regulating development, growth and cell fusion[23–27].

Our previous studies showed that deletion of calponin 2 attenuates the development of inflammatory arthritis[28] and arterial atherosclerosis[29] by restricting macrophage activation. We also demonstrated that the expression and function of calponin 2 is both regulated by the mechanical tissue environment such as stiffness and distension force[19, 20, 30], and the expression of calponin 2 increases during myofibroblast differentiation in aortic valve interstitial cells and its deletion attenuates the fibrocalcification of valves[31]. These findings suggest a hypothesis that calponin 2 may play a role in the development of postoperative peritoneal adhesion through regulating macrophage and fibroblast functions. To test this novel hypothesis, the present study investigated the effects of calponin 2 deletion on the development of postoperative peritoneal adhesion in calponin 2 knockout (KO) mice and underlying cellular mechanisms.

Materials and Methods

Animal Model

All animal experiments were performed under protocols approved by the Institutional Animal Care and Use Committee of Wayne State University. The animals were housed in a temperature and humidity-controlled room with 12-hour light/night cycle and accessed to food and water ad libitum. The development of calponin 2 KO ($Cnn2^{-/-}$) mice has been described previously[32]. The $Cnn2^{-/-}$ and wild type (WT) control mice are both in C57BL/6 strain with comparable genetic background. Genotype of the mice was determined using PCR on tissue biopsies and verified by Western blot analysis[28] of spleen cells post mortem (Figure 1).

Surgical Procedures

Twenty four pairs of 8–10 weeks old male and female calponin 2 KO and WT mice were used in the present study. Sixteen pairs of the mice were randomly selected for the study groups to receive adhesion-causing surgery as described below. Eight pairs of calponin 2 KO and WT mice were used as sham surgery groups. All of the surgeries were performed between 9–11am by the same researcher who is an experienced surgeon with extensive training in performing small animal surgeries. Another researcher performed mouse genotyping, recorded general information and randomly chose the mice for the surgeon to perform either adhesion or sham surgeries in an operator-blinded setting.

Each mouse was given a weight-based dose of intramuscular analgesics one hour before surgery and anesthetized with continuous inhalation of 2% isoflurane and vital signs monitored. All surgical procedures followed standard aseptic techniques and sterilization

protocols. After removing fur and disinfecting the abdominal skin with aqueous iodine solution, a 1.5 cm longitudinal midline incision was made through the abdominal wall from below xyphoid process toward the pelvis.

We followed a previously reported method of surgical induction of peritoneal adhesion[33] with some modifications to mechanically produce a measurable and reproducible area of injury. Briefly, after opening the abdominal cavity the right side abdominal wall was exposed and a 9 mm × 9 mm × 1 mm plastic plate was placed underneath from the skin side to elevate a reproducibly defined area for the application of abrasive injury by manual rubbing of 20 times with a piece of sterile surgical cloth, which produced rough surfaces with petechiae of the parietal layer of the peritoneum without bleeding.

The entire anti-mesenteric serosa surface of the cecum was gently rubbed 20 times with another piece of sterilized cloth to generate surface injury without bleeding or perforation. During the rubbing, the cecum was rinsed several times with sterile saline prewarmed to 37°C to keep the tissue moisturized. The wounded cecum was approximated folding in U-shape as an intent to promote reproducible contacts between the injured surfaces when it was placed back into the left side of abdominal cavity and away from the middle abdominal incision line (Figure 2). Physical approximation has been shown to enhance adhesion formation[34]. The U-shape placement of cecum applies this concept to promote lesion-induced adhesion but avoids using suture to preclude foreign body-induced adhesion formation. Although bowel motility is unavoidable, we used the uniform positioning rather than random positioning to minimize variations. The abdominal wall was closed with sterile surgical clips to avoid suture-induced peritoneal adhesions.

For sham surgery, the mice received the same doses of medication and anesthesia, laparotomy, abdominal exposure, U shape approximated placement of cecum, and clipping of the abdominal wall as the study groups, but without abrasion. The total time of anesthesia and surgery was limited to less than 30 minutes for both study and sham surgery groups. Postoperative animals were individually placed in cages on a heating pad for at least one hour until full activity resumed before returning to the vivarium. The mice received standard postoperative care with daily monitoring of food/water intake, activities, skin wound conditions and weight loss throughout the period of study. The animals were euthanized 3 or 7 days after operation using CO_2 gas followed by cervical dislocation for post-mortem pathoanatomical and pathohistological studies.

Quantification of Cecal Adhesions

The abdominal wall was opened laterally to the original incision to avoid destroying any peritoneal adhesion. Photographs were taken with a ruler for the sites abraded during the original operation to measure the formation and size of adhesions.

A peritoneal adhesion scoring system was applied with modification of a previously described method that scores adhesions based on qualitative assessment such as thin or thick adhesion[35]. Taking advantage that our procedure generates measurable area of injury, we objectively scored the degree of adhesion with the following criteria: 0 = no adhesion, 1 = minimally notable adhesions causing cecal wall contractures, 2 = adhesions formed in less

than 50% of the length of cecum, 3 = adhesions formed in more than 50% of the length of cecum, and 4 = adhesions formed in more than 50% of the length of cecum plus adhesions of cecum to abdominal wall or other organs (Figure 3).

Histological Examinations

Abdominal organs with adhesion formation were excised carefully to avoid separation of the adhered tissues. The entire cecum was cut beyond the joint of small and large intestines together with other organs that it adhered to, if any. The isolated cecum was transversely cut through the adhesion site. Half of the tissue was embedded with the adhesion site facing the cutting plane in a cryomold in Tissue-Tek optimal cutting temperature (O.C.T.) compound (Sakura Finetek USA, Terrance, CA, USA) and rapidly frozen in liquid nitrogen, and stored at −80°C. The frozen O.C.T. tissue blocks were cut into 8 μm thick sections using a ThermoFisher HM550 cryostat. Serial sections were collected on Fisher Superfrost Plus slides and stored at −80°C.

The other half of the cecum were fixed with 4% paraformaldehyde in phosphate-buffered saline (PBS, pH 7.4) overnight and processed for paraffin embedding using standard methods. Serial sections of 4 μm thick were stained with Mayer's Hematoxylin and eosin Y (Electron Microscopy Sciences, 26042) or with Masson Trichrome (Richard-Allen Scientific, 87019) using protocols provided by the manufacturer.

Histological Quantification of Adhesions

The development of adhesions was further quantified at histological level using a bright field light microscope with imaging software (Keyence, BZ-X810). To quantify the adhesion site that are usually in irregular contours in microscopical images, we calculated the area to length ratio (A/L ratio) of the adhesion for comparison between WT and KO groups. This approach allows objective measurements of the average thickness of the proliferative layer in the adhesion formations. To include adhesions formed from abrasive injury of both abdominal wall and cecum, we defined adhesion in microscopic views as an injured site adhered to another injured or a non-injured site to form a continuous tissue band between the underneath muscle layers. The injured sites without connection to another site were not included. The total area of adhesion was calculated as the sum of multiple manually identified geometric sectors in the microscopic image of tissue sections. Using the same criteria described above, the total adhesion area was normalized to the total length of the sectors to obtain the A/L ratio (Figure 4).

The adhesions formed between an injured site with an uninjured site, such as colon or omentum fat, reflect a higher tendency of pathogenesis and were scored by multiplication with a factor of 2 (Figure 4A). This arbitrary normalizing factor for the quantitative comparison is based on the fact that adhesions between the wounded peritonea and unwounded organs were originated from less severe one site injury reflecting a higher tendency of adhesion vs that between two wounded peritoneal surfaces from more severe injuries.

Immunofluorescence Microscopy

The tissue cryosections were air-dried at room temperature for 60 minutes and fixed with ice-cold 75% acetone and 25% ethanol for 10 minutes. Endogenous peroxidase activity was quenched with 1% hydrogen peroxide in PBS at room temperature for 10 minutes. After three washes with PBS, the sections were blocked by incubation with 3% bovine serum albumin (BSA) in PBS for 30 minutes. The sections were then probed with primary antibodies against calponin 2 (RAH2[19]), F4/80 (a mouse macrophage marker) (Abcam, ab6640) and α-smooth muscle actin (α-SMA, a myofibroblast marker) (Sigma A5228) at 4°C overnight. After washing three times with PBS containing 0.05% Tween-20 for 5 minutes each, the sections were incubated with fluorescein isothiocyanate-conjugated goat anti-mouse IgG (Sigma, F1010), tetramethyl rhodamine isothiocyanate (TRITC)-conjugated anti-mouse IgG (Sigma, T-5393) or FITC-conjugated goat anti-rabbit IgG (Sigma, F7512) secondary antibody at room temperature for one hour, washed three times for 5 minutes each as above, mounted with ProLong Gold antifade reagent with DAPI counter stain for nuclei (Molecular Probes by Life Technologies, ThermoFisher Scientific) and sealed with a cover slip using nail polish. The slides were examined using a Keyence epifluorescence microscope (BZ-X810) immediately or after a short storage at −20°C. F4/80 and α-SMA positive cells were counted and normalized to the imaged area for comparison between calponin 2 KO and WT groups.

Statistical Analysis

Statistical analyses were performed with IBM SPSS statistics software (Version 26). Data were presented as mean ± standard deviation (SD). Non-parametric data were shown as median ± interquartile range (IQR). The difference of continuous variables was assessed by using one-way ANOVA with normally distributed data. Mann-Whitney test was used for non-normally distributed continuous data. P value less than 0.05 was considered significant.

Results and Discussion

A Reproduceable Surgical Protocol for the Study of Postoperative Peritoneal Adhesion

All 48 mice survived the operation and the post-surgery period without notable surgery or anesthesia related complications. Less than 10% of body weight loss during the first three days postoperatively was observed, likely due to decreased ambulation that limited the amount of food and water intakes. The mice did not show any asphyxia, bleeding, wound dehiscence or other adverse conditions that require euthanasia and exclusion from the study. The mice all regained their normal body weight in 4–5 days postoperatively. No significant difference in body weight changes was found between calponin 2 KO and WT groups at the end points of experimentation.

Most of histopathological scoring systems in the literature used visual observation to determine the severity of adhesion[33, 36]. Those approaches are often subjective and not easily reproducible by different investigators. Derived from a method described previously[35], our scoring system provides objective quantification of peritoneal adhesions. The results showed tight IQR with few outliers, providing reliable measurements for the severity of postsurgical peritoneal adhesion. Based on the concept that the area of adhesion

is proportional to proliferation of inflammatory and fibrotic cells plus collagen deposition, we further used the A/L ratio of adhesions for a normalized quantification in histological sections to objectively assess the development of fibrotic remodeling underlying the extents of postoperative peritoneal adhesion.

The non-infectious surgical procedure applied in our study reliably and reproducibly generated quantifiable peritoneal adhesions in both WT and $Cnn2^{-/-}$ mice, providing an effective approach to study the effect of calponin 2 deletion on the development of postoperative peritoneal adhesion.

Deletion of Calponin 2 Significantly Reduces Postoperative Peritoneal Adhesion

All sham surgery group of mice did not develop cecal adhesions. Peritoneal adhesion score was assessed and compared between the two study groups on post-surgery Day 3 and Day 7 (Table 1). In comparison with the pathology at postoperative Day 3, formation of adhesion was progressively intensified at postoperative Day 7 in both groups. However, calponin 2 KO mice exhibited significantly lower adhesion score (median = 1.5, IQR = 1.00–2.25) than that of the WT mice (median = 3.5, IQR = 2.75–4.0) on post-surgery Day 3. The significant difference continued to post-surgery Day 7 with adhesion scores of median = 3.0, IQR = 2.75–3.0 for calponin 2 KO and median = 4.0, IQR = 3.0–4.0 for WT.

Normalized quantification of A/L ratio of adhesions in histological sections confirmed the significantly attenuated pathology in calponin 2 KO mice than that in WT mice (Figure 4). The histopathological comparison showed that the average A/L ratio of the adhesions in calponin 2 KO mice was less than half of that of the WT mice (Figure 4A), demonstrating the significant effect of calponin 2 deletion on reducing the formation of postoperative peritoneal adhesion.

Deletion of Calponin2 Attenuates Macrophage Recruitment during Postoperative Peritoneal Wound Healing

F4/80 is a specific marker for mouse macrophages. Immunofluorescent staining of F4/80 on frozen sections of adhesion sites 3 days after surgical lesion showed diffuse infiltration of inflammatory cells in the proliferating mesothelial layer of the adhesion sites and in areas with rich blood supply such as cecal mucosa and submucosal layers. Quantification of macrophage density at adhesion sites found a lower percentage of F4/80+ cells in calponin 2 KO samples than that in WT controls (Figure 5A).

Macrophages are the major cell type orchestrating the inflammatory response during the first three days after tissue injury[10]. Activated macrophages recruited to the injury site release cytokines and other inflammatory mediators to activate fibroblast differentiation into myofibroblasts[37]. While the inflammatory response in postoperative peritoneal injuries also involve other immune cells such as neutrophils and lymphocytes, our previous studies showed that specific deletion of calponin 2 in macrophages effectively attenuates inflammatory arthritis[28] and arterial atherosclerosis[29]. The results of our present study demonstrate that the function of calponin 2 in macrophage activation and inflammatory responses plays an important role in the development of postoperative peritoneal adhesion,

and the deletion of calponin 2 in macrophages may attenuate the initial activation of macrophages to reduce the pathogenesis.

Deletion of Calponin2 Attenuates Myofibroblast Activation during Postoperative Peritoneal Wound Healing

Immunofluorescence microscopy on frozen sections of cecal tissue 7 days after surgical lesion detected α-SMA positive cells accumulated in the deeper layer of adhesion sites. Quantification of the density of α-SMA positive cells showed a lower percentage of α-SMA positive cells in calponin 2 KO samples as compared to WT control (Figure 5B).

After peritoneal tissue injury, the repairing and regeneration process involves fibrotic remodeling and scar formation[3]. Calponin 2 expresses in fibroblasts[21]. Our previous study showed that calponin 2 increases during the differentiation of fibroblasts into myofibroblasts, which plays a critical role in the pathogenesis of aortic valve fibrocalcification[31]. Calponin 2 is not expressed in mesothelial cells whereas the expression of calponin 2 will be turned on in myofibroblasts differentiated from mesothelial cells during trauma-induced MMT. Calponin 2 is an upstream regulator leading myofibroblast differentiation whereas systemic but not macrophage-specific deletion of calponin 2 attenuates myofibroblast differentiation and the development and progression of calcific aortic valve disease[31]. Our present study using a systemic calponin 2 deletion mouse model reproduced the attenuation of myofibroblast differentiation after surgically induced peritoneal injury to minimize the formation of adhesions (Figure 5B).

Calponin 2 expression is mechanically regulated[38]. Mechanical tension and tissue stiffness may contribute to the development and prognosis of postoperative peritoneal adhesion via affecting the expression and function of calponin 2 in various cell types especially myofibroblast differentiation and fibrotic remodeling, which renders calponin 2 an attractive therapeutic target.

Conclusion

The present study provides clear evidence that deletion of calponin 2 effectively attenuates the severity of postoperative peritoneal adhesion through modifying macrophage and fibroblast activities. The results support that calponin 2 plays a role in the pathogenesis of postoperative peritoneal adhesion. This finding opens a translational direction for further research toward the development of a clinical prevention. Reduction of calponin 2 in cells present in and recruited to the injury site by using localized pharmacological approaches may be able to suppress macrophage activation and the downstream activation of myofibroblast differentiation to attenuate peritoneal adhesions. This hypothesis merits continuing research in order to develop a timely needed therapeutic approach to minimize the formation of postsurgical peritoneal adhesions.

Acknowledgements

References

1. van Goor H. Consequences and complications of peritoneal adhesions. Colorectal Dis. Oct 2007;9 Suppl 2:25–34. doi:10.1111/j.1463-1318.2007.01358.x [PubMed: 17824967]

2. Mutsaers SE, Prele CM, Pengelly S, Herrick SE. Mesothelial cells and peritoneal homeostasis. Fertil Steril. Oct 2016;106(5):1018–1024. doi:10.1016/j.fertnstert.2016.09.005 [PubMed: 27692285]

3. Capobianco A, Cottone L, Monno A, Manfredi AA, Rovere-Querini P. The peritoneum: healing, immunity, and diseases. J Pathol. Oct 2017;243(2):137–147. doi:10.1002/path.4942 [PubMed: 28722107]

4. Liakakos T, Thomakos N, Fine PM, Dervenis C, Young RL. Peritoneal adhesions: etiology, pathophysiology, and clinical significance. Recent advances in prevention and management. Dig Surg. 2001;18(4):260–73. doi:10.1159/000050149 [PubMed: 11528133]

5. ten Broek RP, Bakkum EA, Laarhoven CJ, van Goor H. Epidemiology and Prevention of Postsurgical Adhesions Revisited. Ann Surg. Jan 2016;263(1):12–9. doi:10.1097/SLA.0000000000001286 [PubMed: 26135678]

6. Tulandi T, Agdi M, Zarei A, Miner L, Sikirica V. Adhesion development and morbidity after repeat cesarean delivery. Am J Obstet Gynecol. Jul 2009;201(1):56 e1–6. doi:10.1016/j.ajog.2009.04.039 [PubMed: 19576375]

7. Sikirica V, Bapat B, Candrilli SD, Davis KL, Wilson M, Johns A. The inpatient burden of abdominal and gynecological adhesiolysis in the US. BMC Surg. Jun 9 2011;11:13. doi:10.1186/1471-2482-11-13 [PubMed: 21658255]

8. Strik C, Wever KE, Stommel MWJ, Goor HV, Ten Broek RPG. Adhesion reformation and the limited translational value of experiments with adhesion barriers: A systematic review and meta-analysis of animal models. Sci Rep. Dec 3 2019;9(1):18254. doi:10.1038/s41598-019-52457-2 [PubMed: 31796777]

9. Arung W, Meurisse M, Detry O. Pathophysiology and prevention of postoperative peritoneal adhesions. World J Gastroenterol. Nov 7 2011;17(41):4545–53. doi:10.3748/wjg.v17.i41.4545 [PubMed: 22147959]

10. Koninckx PR, Gomel V, Ussia A, Adamyan L. Role of the peritoneal cavity in the prevention of postoperative adhesions, pain, and fatigue. Fertil Steril. Oct 2016;106(5):998–1010. doi:10.1016/j.fertnstert.2016.08.012 [PubMed: 27523299]

11. Jin X, Ren S, Macarak E, Rosenbloom J. Pathobiological mechanisms of peritoneal adhesions: The mesenchymal transition of rat peritoneal mesothelial cells induced by TGF-beta1 and IL-6 requires activation of Erk1/2 and Smad2 linker region phosphorylation. Matrix Biol. Apr 2016;51:55–64. doi:10.1016/j.matbio.2016.01.017 [PubMed: 26825317]

12. Hinz B. Myofibroblasts. Exp Eye Res. Jan 2016;142:56–70. doi:10.1016/j.exer.2015.07.009 [PubMed: 26192991]

13. Abe M, Takahashi K, Hiwada K. Effect of calponin on actin-activated myosin ATPase activity. J Biochem. Nov 1990;108(5):835–8. doi:10.1093/oxfordjournals.jbchem.a123289 [PubMed: 2150518]

14. Winder SJ, Walsh MP. Smooth muscle calponin. Inhibition of actomyosin MgATPase and regulation by phosphorylation. J Biol Chem. Jun 15 1990;265(17):10148–55. [PubMed: 2161834]

15. Haeberle JR. Calponin decreases the rate of cross-bridge cycling and increases maximum force production by smooth muscle myosin in an in vitro motility assay. J Biol Chem. Apr 29 1994;269(17):12424–31. [PubMed: 8175648]

16. Jin JP, Zhang Z, Bautista JA. Isoform diversity, regulation, and functional adaptation of troponin and calponin. Crit Rev Eukaryot Gene Expr. 2008;18(2):93–124. doi:10.1615/critreveukargeneexpr.v18.i2.10 [PubMed: 18304026]

17. Liu R, Jin JP. Calponin isoforms CNN1, CNN2 and CNN3: Regulators for actin cytoskeleton functions in smooth muscle and non-muscle cells. Gene. Jul 1 2016;585(1):143–153. doi:10.1016/j.gene.2016.02.040 [PubMed: 26970176]

18. Hossain MM, Hwang DY, Huang QQ, Sasaki Y, Jin JP. Developmentally regulated expression of calponin isoforms and the effect of h2-calponin on cell proliferation. Am J Physiol Cell Physiol. Jan 2003;284(1):C156–67. doi:10.1152/ajpcell.00233.2002 [PubMed: 12388067]

19. Nigam R, Triggle CR, Jin JP. h1- and h2-calponins are not essential for norepinephrine- or sodium fluoride-induced contraction of rat aortic smooth muscle. J Muscle Res Cell Motil. Aug 1998;19(6):695–703. doi:10.1023/a:1005389300151 [PubMed: 9742453]

20. Feng HZ, Wang H, Takahashi K, Jin JP. Double deletion of calponin 1 and calponin 2 in mice decreases systemic blood pressure with blunted length-tension response of aortic smooth muscle. J Mol Cell Cardiol. Apr 2019;129:49–57. doi:10.1016/j.yjmcc.2019.01.026 [PubMed: 30707993]

21. Hossain MM, Crish JF, Eckert RL, Lin JJ, Jin JP. h2-Calponin is regulated by mechanical tension and modifies the function of actin cytoskeleton. J Biol Chem. Dec 23 2005;280(51):42442–53. doi:10.1074/jbc.M509952200 [PubMed: 16236705]

22. Hossain MM, Smith PG, Wu K, Jin JP. Cytoskeletal tension regulates both expression and degradation of h2-calponin in lung alveolar cells. Biochemistry. Dec 26 2006;45(51):15670–83. doi:10.1021/bi061718f [PubMed: 17176089]

23. Applegate D, Feng W, Green RS, Taubman MB. Cloning and expression of a novel acidic calponin isoform from rat aortic vascular smooth muscle. J Biol Chem. Apr 8 1994;269(14):10683–90. [PubMed: 8144658]

24. Li Z, Jackson M, Deslauriers R, Ye J. Unclamping the inferior vena cava during retrograde cerebral perfusion increases the safe range of retrograde perfusion pressures and improves brain perfusion. Interact Cardiovasc Thorac Surg. Jun 2004;3(2):265–9. doi:10.1016/j.icvts.2003.12.001 [PubMed: 17670232]

25. Shibukawa Y, Yamazaki N, Kumasawa K, et al. Calponin 3 regulates actin cytoskeleton rearrangement in trophoblastic cell fusion. Mol Biol Cell. Nov 15 2010;21(22):3973–84. doi:10.1091/mbc.E10-03-0261 [PubMed: 20861310]

26. Trabelsi-Terzidis H, Fattoum A, Represa A, Dessi F, Ben-Ari Y, der Terrossian E. Expression of an acidic isoform of calponin in rat brain: western blots on one- or two-dimensional gels and immunolocalization in cultured cells. Biochem J. Feb 15 1995;306 (Pt 1):211–5. doi:10.1042/bj3060211 [PubMed: 7864813]

27. Flemming A, Huang QQ, Jin JP, Jumaa H, Herzog S. A Conditional Knockout Mouse Model Reveals That Calponin-3 Is Dispensable for Early B Cell Development. PLoS One. 2015;10(6):e0128385. doi:10.1371/journal.pone.0128385 [PubMed: 26046660]

28. Huang QQ, Hossain MM, Sun W, Xing L, Pope RM, Jin JP. Deletion of calponin 2 in macrophages attenuates the severity of inflammatory arthritis in mice. Am J Physiol Cell Physiol. Oct 1 2016;311(4):C673–C685. doi:10.1152/ajpcell.00331.2015 [PubMed: 27488671]

29. Liu R, Jin JP. Deletion of calponin 2 in macrophages alters cytoskeleton-based functions and attenuates the development of atherosclerosis. J Mol Cell Cardiol. Oct 2016;99:87–99. doi:10.1016/j.yjmcc.2016.08.019 [PubMed: 27575021]

30. Liu R, Hossain MM, Chen X, Jin JP. Mechanoregulation of SM22alpha/Transgelin. Biochemistry. Oct 17 2017;56(41):5526–5538. doi:10.1021/acs.biochem.7b00794 [PubMed: 28898058]

31. Plazyo O, Liu R, Moazzem Hossain M, Jin JP. Deletion of calponin 2 attenuates the development of calcific aortic valve disease in ApoE(−/−) mice. J Mol Cell Cardiol. Aug 2018;121:233–241. doi:10.1016/j.yjmcc.2018.07.249 [PubMed: 30053524]

32. Huang QQ, Hossain MM, Wu K, Parai K, Pope RM, Jin JP. Role of H2-calponin in regulating macrophage motility and phagocytosis. J Biol Chem. Sep 19 2008;283(38):25887–99. doi:10.1074/jbc.M801163200 [PubMed: 18617524]

33. Kraemer B, Wallwiener C, Rajab TK, Brochhausen C, Wallwiener M, Rothmund R. Standardised models for inducing experimental peritoneal adhesions in female rats. Biomed Res Int. 2014;2014:435056. doi:10.1155/2014/435056 [PubMed: 24809049]

34. Poehnert D, Abbas M, Kreipe HH, Klempnauer J, Winny M. High reproducibility of adhesion formation in rat with meso-stitch approximation of injured cecum and abdominal wall. Int J Med Sci. 2015;12(1):1–6. doi:10.7150/ijms.8870 [PubMed: 25552912]

35. Yang YL, Lee MG, Lee CC, et al. Pentoxifylline decreases post-operative intra-abdominal adhesion formation in an animal model. PeerJ. 2018;6:e5434. doi:10.7717/peerj.5434 [PubMed: 30155353]

36. Whang SH, Astudillo JA, Sporn E, et al. In search of the best peritoneal adhesion model: comparison of different techniques in a rat model. J Surg Res. May 15 2011;167(2):245–50. doi:10.1016/j.jss.2009.06.020 [PubMed: 20304431]

37. Namvar S, Woolf AS, Zeef LA, Wilm T, Wilm B, Herrick SE. Functional molecules in mesothelial-to-mesenchymal transition revealed by transcriptome analyses. J Pathol. Aug 2018;245(4):491–501. doi:10.1002/path.5101 [PubMed: 29774544]

38. Jiang WR, Cady G, Hossain MM, Huang QQ, Wang X, Jin JP. Mechanoregulation of h2-calponin gene expression and the role of Notch signaling. J Biol Chem. Jan 17 2014;289(3):1617–28. doi:10.1074/jbc.M113.498147 [PubMed: 24285540]
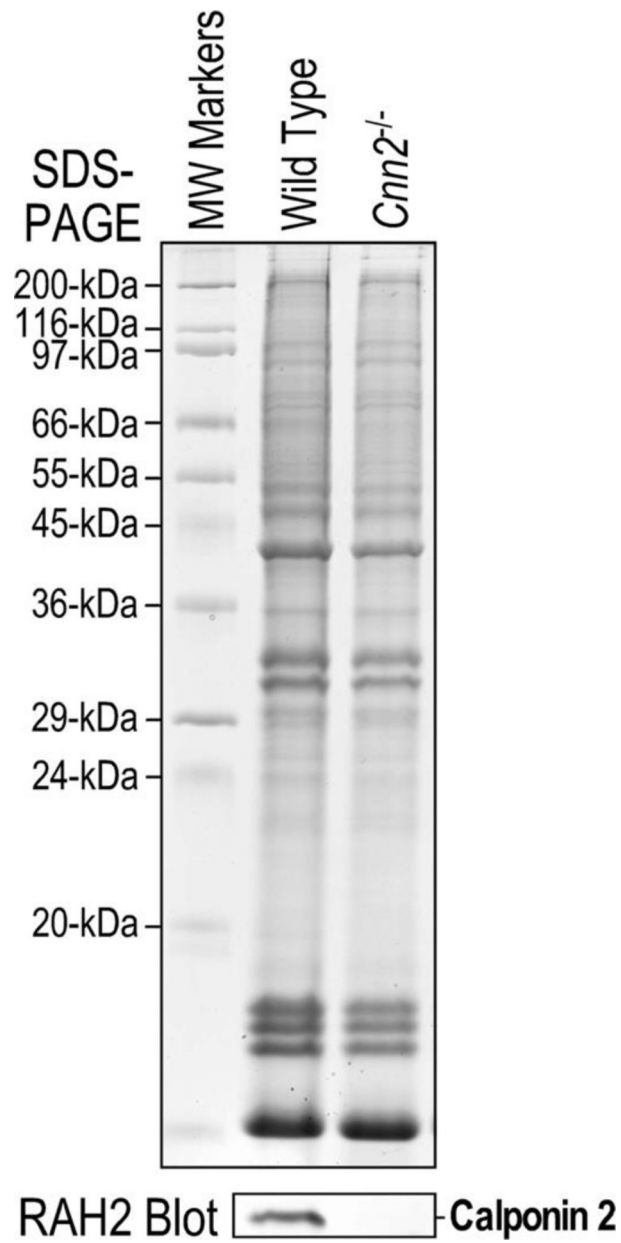
Figure 1. Western blot conformation of *Cnn2* KO mice.
12% SDS-polyacrylamide gel of total protein extract from spleen tissue and Western blot of a replica gel using an anti-calponin2 antibody RAH2[19] confirmed the complete deletion of calponin 2 in *Cnn2*^{−/−} mice. Wild type (WT) mouse spleen was used as control.

Figure 2. Surgical induction of peritoneal adhesions.
A. An area defined using an underneath 9 mm × 9 mm metal plate was abraded, producing a rough surface with mild petechiae without bleeding or oozing. B. The entirely abraded cecum showing a rough surface of the visceral peritoneum was folded to make contact between the injured surfaces before replacement into the abdominal cavity.
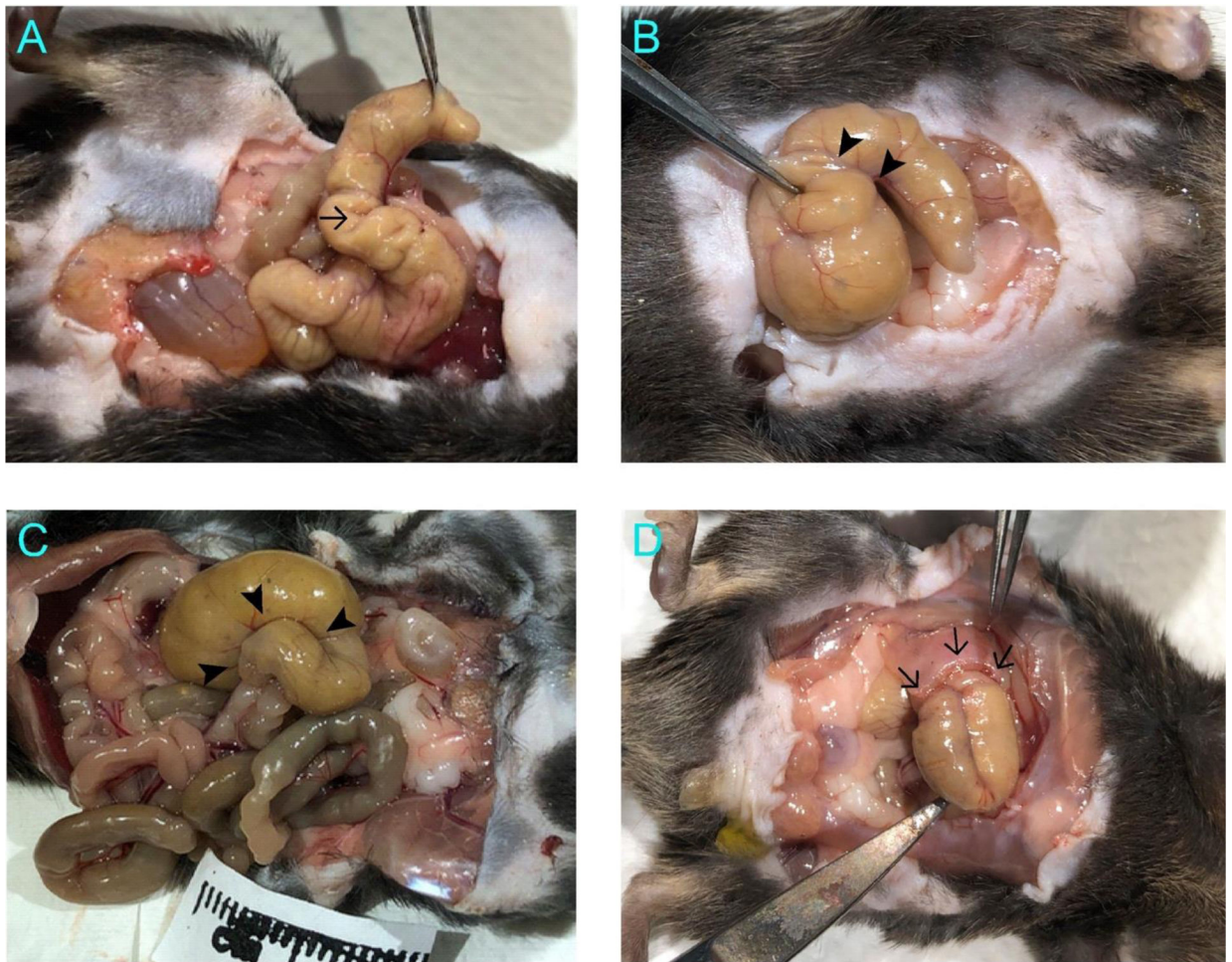
Figure 3. Examples of scored cecal adhesions.
A. Score 1 represents minimal adhesions causing cecal wall contractures such as that pointed by the arrow. B. Score 2 corresponds to adhesions formed in less than 50% of the cecum length such as that between the two arrowheads. C. Score 3 is for adhesions formed in more than 50% of the cecum length such as the region outlined by the three arrowheads corresponding to ~90% of the cecum length. D. Score 4 indicates additional adhesions between cecum and abdominal wall or other organs. The arrows indicate adhesions formed between cecum and abdominal wall.

A/L Ratio

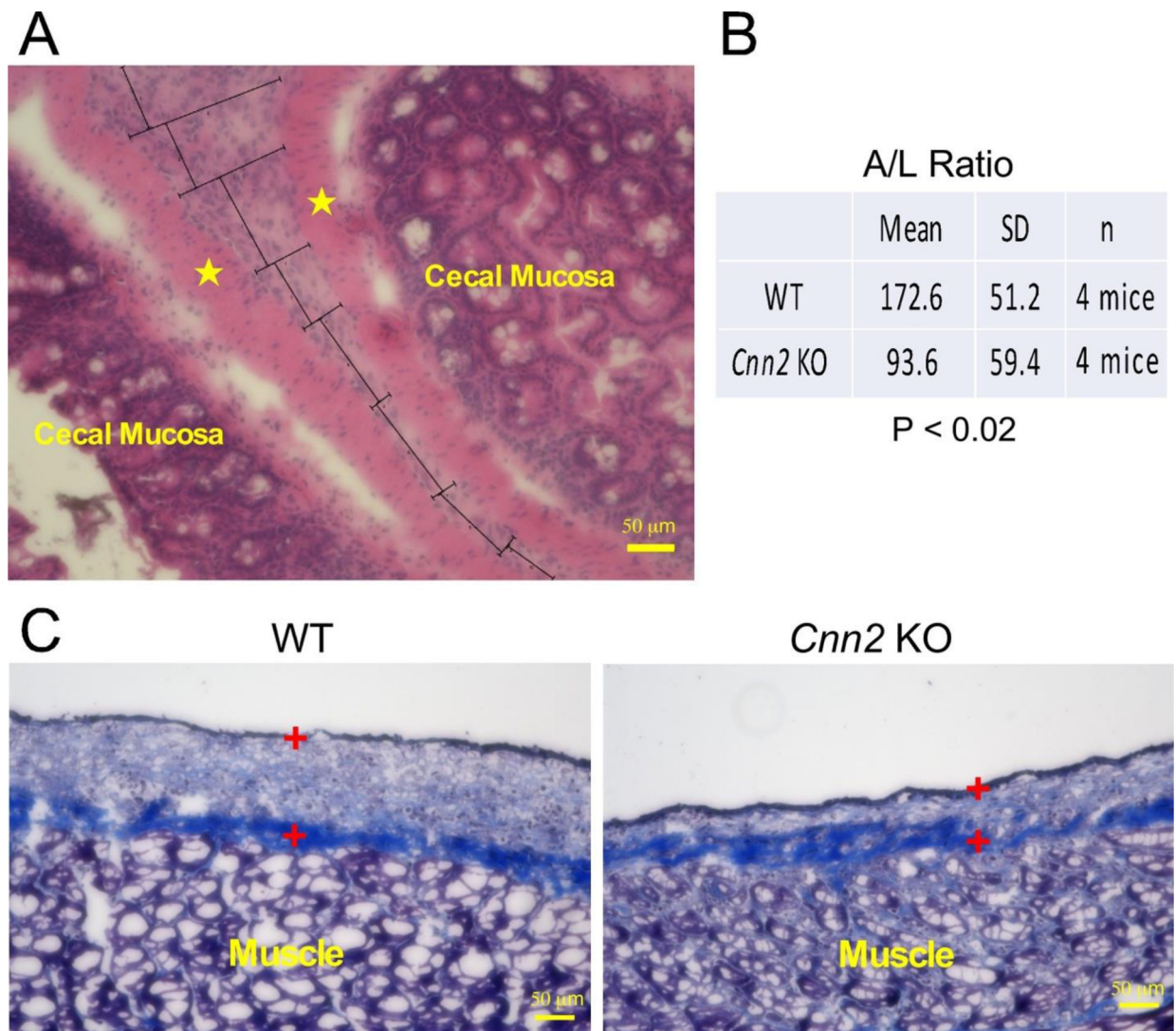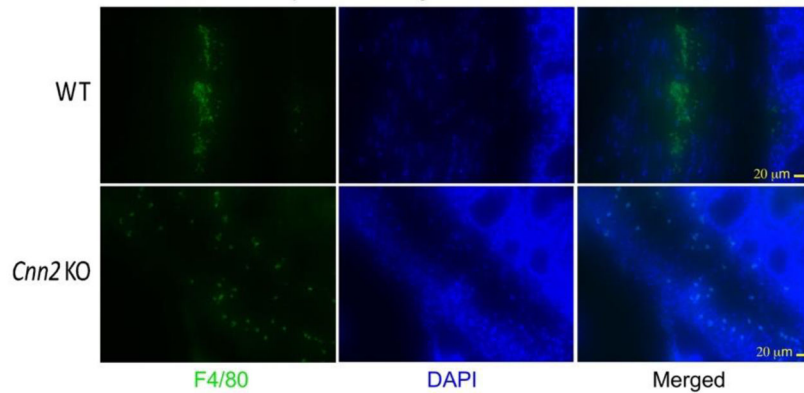|	Mean	SD	n
WT	172.6	51.2	4 mice
Cnn2 KO	93.6	59.4	4 mice

$P < 0.02$

Figure 4: Deletion of calponin 2 minimizes the formation of proliferating mesothelial layer and collagen deposition in postoperative Day 7 peritoneal adhesions.

(A) A cross section of a representative Day 7 WT cecal adhesion site showing proliferating mesothelial cells between muscle layers (indicated by the stars) of the cecal walls was used to illustrate the calculation of A/L ratio in the tissue sections. The adhesion image was divided geometrically and the total area containing mesothelial cells measured using a computer software was divided by the total length of adhesion. (B) Quantitative analysis of the A/L ratio showed that *Cnn2* KO mice had a significantly lower A/L ratio than WT control. (C) Cross sections of a Day 7 abdominal wall abrasive site revealed that collagen deposition in Masson's Trichrome stain mainly located in the deeper layer of the proliferating mesothelial layer, which was less in calponin 2 KO than that in WT control (the proliferating mesothelial cell layer was marked by the two + symbols).
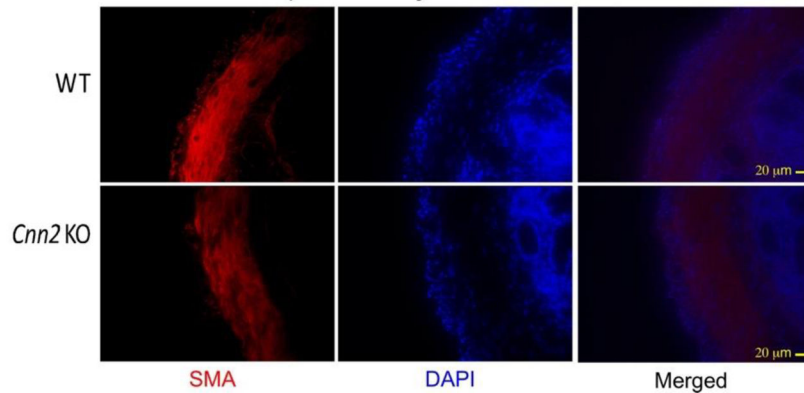
A F4/80⁺ Cells at Postoperative Day 3

F4/80⁺/Total Cells			
	Mean	SD	n
WT	15.2%	1.8%	4 mice
Cnn2 KO	5.5%	0.8%	4 mice
	$P < 0.001$		

B SMA⁺ Cells at Postoperative Day 7

SMA⁺/Total Cells			
	Mean	SD	n
WT	19.2%	1.4%	4 mice
Cnn2 KO	5.3%	1.4%	4 mice
	$P < 0.001$		

Figure 5: Calponin 2 KO mice exhibit attenuated macrophage infiltration and myofibroblast differentiation during the healing of operational injuries.

(A) Immunofluorescence micrographs of thin sections of cecal adhesion sites at postoperative Day 3 showed significantly less infiltration of F4/80⁺ macrophages (green) in calponin 2 KO mice in comparison with that of wild type controls. (B) At postoperative Day 7, immunofluorescence microscopy further showed significantly less α-SMA-positive (red) myofibroblasts in sections of cecal adhesion sites from calponin 2 KO mice than that in WT control. DAPI nucleus stain (blue) was used to identify the total number of cells.

Table 1.

Calponin 2 KO mice developed significantly less postoperative peritoneal adhesions than WT controls

	POD3		POD7	
	WT	**KO**	**WT**	**KO**
N	8	8	8	8
Mean	3.25	1.75	3.63	2.75
Median	3.50	1.50	4.00	3.00
S.D.	0.89	0.89	0.52	0.46
Range	2.00–4.00	1.00–3.00	3.00–4.00	2.00–3.00
Q1	2.75	1.00	3.00	2.75
Q3	4.00	2.25	4.00	3.00
IQR	1.25	1.25	1.00	0.25
P value	<0.02[*]		<0.02[*]	

At Day 3 (POD3) and Day 7 (POD7) after surgical injury, the data presented as median and interquartile range between 25th and 75th percentile (IQR) showed significantly milder formation of postoperative peritoneal adhesion in calponin 2 KO mice in comparison to that of WT mice.

[*] Statistical analysis was performed using nonparametric Mann Whitney-U test.